BACHELOR

Tractor semi-trailer model validation for low speed maneuvering

Nounou, Youssof Mohamed Abdelhamid

Award date:
2022

Tractor semi-trailer model validation for low speed maneuvering

Department of Mechanical Engineering

Dynamics & control group

BEP Report

Full name	Student ID	Study
Youssof Nounou	1458515	Mechanical Engineering

Supervisors
Dr. Ir. I.J.M. Besselink
Ing. V.V. Gosar MSc

Eindhoven, July 8, 2022

Abstract

In this research, a kinematic vehicle model of a tractor semi-trailer vehicle is analyzed. The main goals are to extend the current model, evaluate and improve it. The model is validated using real world measurement data that was collected by doing experiments with a real vehicle. In these experiments, the sensors recorded different signals like position, velocity and acceleration. The model should therefore be extended with the same signals that the sensors measure so that a proper comparison can be made.

One of the questions that should arise from this is whether the measurement data is actually reliable or not. That is why the model is used to verify the measurement data first. From this verification it is found that there are some signals that showed large deviations from the model results. For most of these signals an explanation was found as to why this was the case and they were corrected. However, an explanation could not be found as to why the wheel velocities show large deviations from the model.

An analysis is made on whether adding load to the vehicle in the measurement data affects the model's accuracy. It is found that the model best represents the loaded configuration. The reason for this was investigated and it was found that it is caused by the fact that when a load is added to the vehicle, this changes the wheelbase of the semi-trailer.

It is known that a tractor semi-trailer vehicle is unstable during reversing because then the articulation angle increases exponentially when a small steering angle is applied. This is demonstrated and a solution for stabilizing the vehicle during reversing is found to be using a proportional controller. The results show that the controller ensures stability of the vehicle when reversing. In addition to that, it also improves its path tracking performance.

Contents

Abstract **1**

List of Symbols **3**

1 Introduction **4**

2 Kinematic Vehicle Model **5**
2.1 Introduction . . . 5
2.2 Extending the model . . . 6
2.3 Asymmetric steering system . . . 7
2.4 Error criteria . . . 7
2.5 Error normalization . . . 9

3 Forward Driving analysis **11**
3.1 Data verification . . . 11
3.2 Animation tool . . . 14
3.3 Loaded and unloaded vehicle configurations . . . 15
3.4 Tuning the steering system parameters . . . 16
3.5 Assessing the model accuracy . . . 18

4 Reverse Driving Analysis **19**
4.1 Reverse driving stability . . . 19
4.2 Reverse driving controller . . . 19
4.3 Tuning the controller . . . 21

5 Conclusion & Recommendations **23**
5.1 Conclusion . . . 23
5.2 Recommendations . . . 23

References **25**

Appendices **26**

A Semi-trailer Equations **26**

B Acceleration contribution **27**

C Error Criteria Extra Plots **28**

D Verifying Measurement Data Extra Plots **29**

E Loaded and Unloaded Vehicle Configurations Comparisons **30**

F Plots for Assessing the Model Accuracy **31**

G Simulink Model **34**

List of Symbols

Symbol	Description	Unit
a	Coefficient of the quadratic term δ^2 in the steering input coefficient	$-$
a_x	Longitudinal acceleration	m/s^2
a_y	Lateral acceleration	m/s^2
e	Error	$-$
g	Gravitational acceleration constant	m/s^2
i_{steer}	Steering ratio	$-$
l	Length	m
v_x	Local longitudinal velocity	m/s
v_y	Local lateral velocity	m/s
x	Global longitudinal position	m
$\dot{x}$	Global longitudinal velocity	m/s
y	Global lateral position	m
$\dot{y}$	Global lateral velocity	m/s
γ	Articulation angle	rad
$\dot{\gamma}$	Articulation angular velocity	rad/s
δ	Front wheel angle	rad
$\dot{\delta}$	Front wheel angular velocity	rad/s
δ^*	Steering wheel angle	rad
ϵ	Error criterion	$-$
ϕ	Roll angle	rad
ψ	Yaw angle	rad
$\dot{\psi}$	Yaw velocity	rad/s
$\ddot{\psi}$	Yaw acceleration	rad/s^2

1 Introduction

There is an aim to automate the driving task of tractor semi-trailer vehicles at distribution centers. This is useful, as it can reduce the docking time and help in avoiding accidents. However, before this can be realized, is is vital to get an understanding of the motions of the vehicle and to be able to predict its movements. This can be done with a kinematic vehicle model.

A kinematic model of a tractor semi-trailer vehicle has been developed, improved and evaluated using real world measurement data [1]. This measurement data was collected at the DPD distribution center in Oirschot, where driving maneuvers that typically occur at a distribution center were performed. The vehicle was equipped with multiple sensors that measure various quantities. The measurement data covers multiple driving maneuvers. Some of the measurements were done with the vehicle being loaded and some were done with the vehicle being unloaded [1].

Despite the fact that some analysis was already done on the model, there are still several aspects that need to be analyzed and improved. The first task is to extend the model with new signals to allow a full comparison between the model and the measurement data. The second task is to develop error criteria that quantify the differences between the model and the measurement data. The third task is to develop an animation tool that showcases the measured trajectories. The fourth task is to analyze the differences between loaded and unloaded vehicle configurations. The fifth task is to analyze the model's performance using the measurement data. The final task is to stabilize the vehicle when driving backwards.

This report is assigned as follows. In chapter two, the kinematic vehicle model is introduced, extended and error criteria are defined. In chapter three, forward driving of the vehicle is analyzed by checking for potentially incorrect measured signals, analyzing the differences between loaded and unloaded vehicle configurations and assessing the model's accuracy. In chapter four, the reverse driving of the vehicle is analyzed with regards to instability when driving backwards and a controller is proposed to stabilize the modeled vehicle when reversing. Finally, conclusions and recommendations are given in chapter five.

2 Kinematic Vehicle Model

In this chapter the model is introduced and extended with additional signals for a detailed comparison with the measurement data. The asymmetric steering system is explained. Error criteria are defined to quantify the performance of the model.

2.1 Introduction

The kinematic vehicle model is derived with the assumption that no side slip of the tires occurs on the tractor and on the center semi-trailer axle. This means that the first and third semi-trailer axles are neglected. The kinematic model can be seen in Figure 2.1.

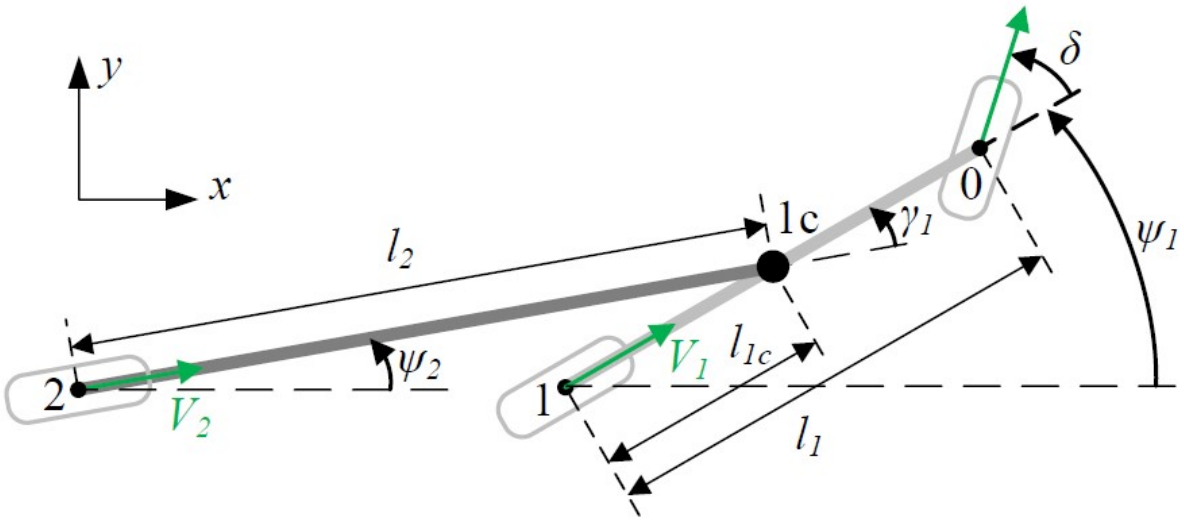

Figure 2.1: Kinematic model representation [2]

The model has two inputs, the first one is the longitudinal velocity of the tractor V_1 and the other one is the steering wheel angle δ. The steering wheel angle δ_h needs to be converted to the front wheel angle. This is done using the steering ratio i_{steer}, as is defined in (2.1). It indicates how many angle rotations in degrees of the steering wheel are needed to give one degree of rotation in the front wheel.

$$\delta = \frac{\delta_h}{i_{steer}} \tag{2.1}$$

From the two inputs to the model, the global velocities v_{x1} and v_{y1} as well as the yaw angle velocities $\dot{\psi}_1$ and $\dot{\psi}_2$ are computed. They are integrated to obtain the global position of the tractor rear axle x_1 and y_1 and the yaw angles of the vehicle ψ_1 and ψ_2. From the yaw angles, the articulation angle γ_1 is computed, which is the difference in yaw angle between the tractor and the semi-trailer. From these quantities, the longitudinal velocity of the semi-trailer V_2 is computed. The positions of the vehicle are found using geometry [1], [2]. The equations are implemented into MATLAB, where the model equations are evaluated in a function. The equations for the described variables are given below.

$$v_{x1} = V_1 \cos(\psi_1) \tag{2.2}$$

$$v_{y1} = V_1 \sin(\psi_1) \tag{2.3}$$

$$\dot{\psi}_1 = \frac{V_1 \tan(\delta)}{l_1} \tag{2.4}$$

$$V_2 = V_1 \cos(\gamma_1) - \dot{\psi}_1 l_{1c} \sin(\gamma_1) \tag{2.5}$$

$$\dot{\psi}_2 = \frac{V_1 \sin(\gamma_1) + \dot{\psi}_1 l_{1c} \cos(\gamma_1)}{l_2} \tag{2.6}$$

2.2 Extending the model

The sensors measure various signals including positions, velocities, accelerations, angles, angular velocities and angular accelerations. These signals also need to be computed in the model. These signals are dependent on each other and can be computed subsequently. Therefore, the approach that is taken is to start with the position, which is already available in the model. The position is differentiated with respect to time to get the velocity. Then the velocity is also differentiated with respect to time to obtain the acceleration and using the velocity and acceleration, the angular accelerations can also be obtained. The yaw angles and yaw velocities are already available in the model. This procedure is demonstrated in the equations below for the tractor. The same procedure is followed for the semi-trailer, it can be seen in Appendix A.

The positions of the tractor axles and the center semi-trailer axle are available in the model; however, the OxTS sensors are mounted at different locations on the vehicle [1]. Therefore, the positions of the OxTS sensors need to be calculated in the model. This is done by shifting the model positions that are available to the sensor positions

$$\begin{bmatrix} x_{1_{OxTS}} & y_{1_{OxTS}} \end{bmatrix} = \begin{bmatrix} x_0 & y_0 \end{bmatrix} + \begin{bmatrix} l_{x1} & l_{y1} \end{bmatrix} \begin{bmatrix} \cos(\psi_1) & \sin(\psi_1) \\ \sin(\psi_1) & -\cos(\psi_1) \end{bmatrix} \tag{2.7}$$

where $x_{1_{OxTS}}$ and $y_{1_{OxTS}}$ are the global coordinates of the position of the OxTS sensor that is mounted on the tractor in the model, x_0 and y_0 are the coordinates of the tractor front axle position in the model and l_{x1} and l_{y1} are the longitudinal and lateral lengths respectively between the tractor front axle and the sensor that is mounted on the tractor.

From the position, the global velocity at the OxTS sensors is calculated by taking the derivative of the position expression. The resulting expression reads

$$\begin{bmatrix} \dot{x}_{1_{OxTS}} & \dot{y}_{1_{OxTS}} \end{bmatrix} = \begin{bmatrix} \dot{x}_0 & \dot{y}_0 \end{bmatrix} + \begin{bmatrix} l_{x1} & l_{y1} \end{bmatrix} \begin{bmatrix} -\sin(\psi_1)\dot{\psi}_1 & \cos(\psi_1)\dot{\psi}_1 \\ \cos(\psi_1)\dot{\psi}_1 & \sin(\psi_1)\dot{\psi}_1 \end{bmatrix} \tag{2.8}$$

where $\dot{x}_{1_{OxTS}}$ and $\dot{y}_{1_{OxTS}}$ are the global velocities in x and y directions respectively at the tractor OxTS sensor and $\dot{x}_0$ and $\dot{y}_0$ are the derivatives of the tractor front axle position coordinates x_0 and y_0 respectively. The magnitude of the global velocity is also calculated for comparison with the measurement data.

In addition to the global velocity, the sensors also measure the local velocity, which is the velocity in the longitudinal and lateral axes of the vehicle in the body fixed frame of the vehicle. This is calculated in the model by converting the global coordinate frame to the local vehicle coordinate frame using a rotation matrix. This can be seen in (2.9)

$$\begin{bmatrix} V_{x1_{OxTS}} & V_{y1_{OxTS}} \end{bmatrix} = \begin{bmatrix} \dot{x}_{1_{OxTS}} & \dot{y}_{1_{OxTS}} \end{bmatrix} \begin{bmatrix} \cos(\psi_1) & -\sin(\psi_1) \\ \sin(\psi_1) & \cos(\psi_1) \end{bmatrix} \tag{2.9}$$

where $V_{x1_{OxTS}}$ and $V_{y1_{OxTS}}$ are the local longitudinal and lateral velocities respectively at the OxTS sensors and the matrix containing $\cos(\psi_1)$ and $\sin(\psi_1)$ is the rotation matrix. The procedure for calculating the local velocity at the OxTS sensors starting from the position is also repeated for the Corrsys sensor to obtain the local velocity at the location where the Corrsys sensor is mounted.

From the local velocity, the acceleration is calculated. The sensors only measure the acceleration in the local frame. The longitudinal and lateral accelerations both have two contributions. The effect of these contributions towards the total acceleration can be seen in Appendix B.

$$\begin{bmatrix} a_{x1_{OxTS}} & a_{y1_{OxTS}} \end{bmatrix} = \begin{bmatrix} \dot{V}_{x1_{OxTS}} & \dot{V}_{y1_{OxTS}} \end{bmatrix} + \begin{bmatrix} -V_{y1_{OxTS}} & V_{x1_{OxTS}} \end{bmatrix} \dot{\psi}_1 \tag{2.10}$$

where $a_{x1_{OxTS}}$ and $a_{y1_{OxTS}}$ are the local longitudinal and lateral accelerations respectively of the tractor, $\dot{V}_{x1_{OxTS}}$ and $\dot{V}_{y1_{OxTS}}$ are the time derivative of the tractor velocity signals in longitudinal and lateral directions respectively.

Using the acceleration and the local velocity, the yaw acceleration of the tractor and semi-trailer are calculated. This is done by taking the time derivative of the yaw velocity expressions that were given in (2.4) and (2.6). The resulting expression reads

$$\ddot{\psi}_1 = \frac{\dot{v}_{x1} \tan(\delta) + v_{x1} \sec^2(\delta)\dot{\delta}}{l_1} \tag{2.11}$$

where $\ddot{\psi}_1$ is the yaw acceleration of the tractor, v_{x1} is the longitudinal velocity of the tractor, $\dot{v}_{x1}$ is the time derivative of the v_{x1} signal, $\dot{\delta}$ is the front wheel angular velocity. The semi-trailer yaw acceleration is given by

$$\ddot{\psi}_2 = \frac{\dot{v}_{x1} \sin(\gamma_1) + v_{x1} \cos(\gamma_1)\dot{\gamma}_1 + \ddot{\psi}_1 l_{1c} \cos(\gamma_1) - \dot{\psi}_1 l_{1c} \sin(\gamma_1)\dot{\gamma}_1}{l_2} \tag{2.12}$$

where $\ddot{\psi}_2$ is the yaw acceleration of the semi-trailer and $\dot{\gamma}_1$ is the articulation angle velocity.

The wheel velocities of the tractor are also calculated in the model. This is done by calculating the positions of the wheels by shifting one of the axle positions to the wheel positions similar to (2.7) using the track width, which is the length between two wheels in an axle. The derivative of the wheel positions is then taken to obtain the global wheel velocities as in (2.8). After which the global velocity is converted to local velocity using the rotation matrix as in (2.9), to obtain the longitudinal wheel velocity. The front wheels of the tractor need to again be converted to the local frame of the wheel because the front wheels are steered with an angle δ.

2.3 Asymmetric steering system

In (2.1), it is shown how the steering ratio is used to obtain the front wheel angle δ. However, there is also an additional term that should be included in the steering input. In a tractor, the steering wheel controls the front left wheel. This causes the left front wheel and the right front wheel to have different steering angles, so the vehicle has asymmetric steering. This is known as Ackermann steering. In the model the steering input is given at the center of the front axle. However, since both front wheels do not have the same angle, it would not be sufficient to model this steering input as a linear term. Instead, a quadratic polynomial term is added. The steering input is given by

$$\delta = \frac{1}{i_{steer}}(\delta_h + a{\delta_h}^2) \tag{2.13}$$

where i_{steer} and a are two important parameters that are tuned and optimized in section 3.

2.4 Error criteria

For an objective comparison between the model and the measurement data, error criteria need to be defined. It is not always easy to judge the error by usual inspection of graphs because in some cases the margin for error might be really small. Error criteria are defined for the position, the velocity, the acceleration, the angle and the angular velocity.

The error criteria are split into two parts. The first part formulates error criteria for the position, velocity and acceleration, while the other part formulates error criteria for the angle and angular velocity. For the first part, the magnitude of these variables is computed for the model and for the measurement data (2.14). The magnitude is taken, because it gives an indication about the error of both longitudinal and lateral

components. Then the absolute difference is found between the modeled magnitude and the measured magnitude (2.15). Finally, to obtain one error value at the end, the mean of the absolute difference of magnitudes is taken (2.16). The error criteria for the position, velocity and acceleration are only used for the semi-trailer. This is because the semi-trailer variables depend on the tractor variables and the tractor computations come directly from the input to the model. Therefore, the semi-trailer variables are prone to have larger errors, which is why they are chosen. This procedure is demonstrated below for the position.

$$p = \sqrt{x^2 + y^2} \tag{2.14}$$

$$e_p = |p_{modeled} - p_{measured}| \tag{2.15}$$

$$\epsilon_p = \bar{e}_p \tag{2.16}$$

Where p is the position magnitude, e_p is the absolute difference of the modeled and measured position magnitudes and ϵ_p is the position error, which is the mean of e_p.

To get a better insight, the position magnitude as well as the magnitude of the error are plotted for a random dataset. They can be seen in Figure 2.2 and Figure 2.3. Furthermore, the value of the error criterion itself is also computed.

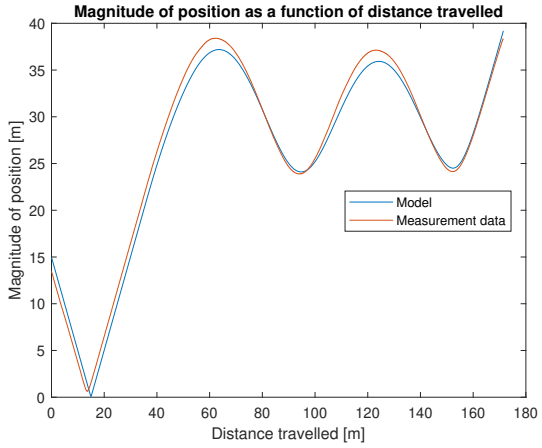

Figure 2.2: Position magnitude

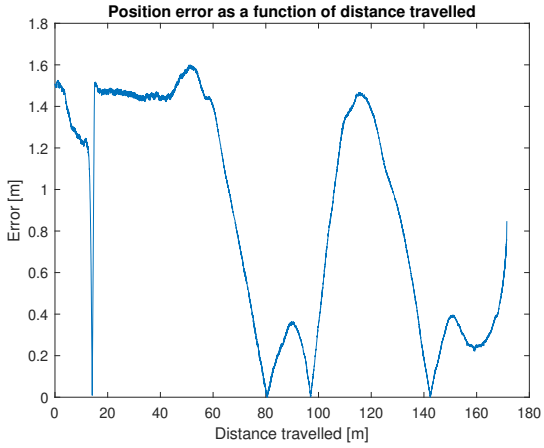

Figure 2.3: Magnitude of position error

The value for the average position error can be seen in Table 2.1. It is concluded that this error criterion is a good method to judge the difference between the model and the measurement data. The same type of plots for the velocity and the acceleration can be found in Appendix C. Their average error values can be seen in Table 2.1.

The second part of the error criteria deals with the angular errors. The only difference is that the magnitude is not taken, because angles and angular velocities only have one component. Therefore, for the angular error criteria, the procedure starts by computing the magnitude difference of the angle or angular velocity. For the articulation angle the error is defined by

$$e_{\gamma_1} = |\gamma_{1_{modeled}} - \gamma_{1_{measured}}| \tag{2.17}$$

$$\epsilon_{\gamma_1} = \bar{e}_{\gamma_1} \tag{2.18}$$

Like with the position, the articulation angle as well as the magnitude of the articulation angle error are plotted. They can be seen in Figure 2.4 and Figure 2.5. Furthermore, the average error is calculated.

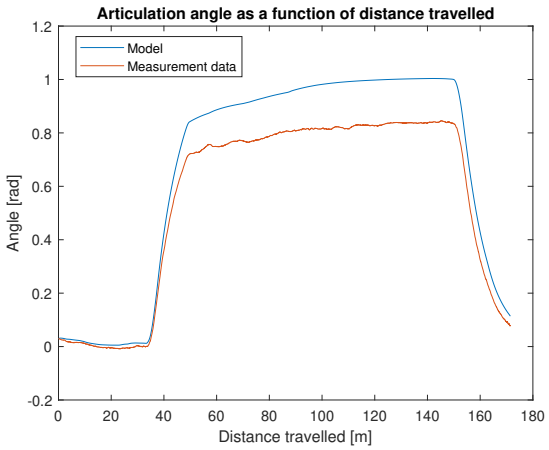

Figure 2.4: Articulation angle

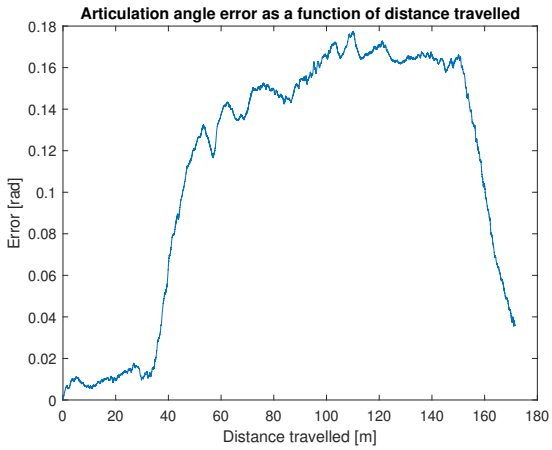

Figure 2.5: Magnitude of articulation angle error

The value of the articulation angle error criterion for this dataset can be seen in Table 2.1. This value seems representative of the total error, as it gives good indication of the whole error of each variable with one error value. It is concluded that the average error criterion is good to use for comparison between the model and the measurement data. The same type of plots for the yaw angles, yaw velocity and articulation angle velocity can be found in Appendix C. Their error criteria values can be seen in Table 2.1.

2.5 Error normalization

It is important to also be able to combine these errors, in order to be able to judge the model accuracy for each dataset with a single number. However, there are two main issues with this. The first one is that not all errors have the same units, so it is not possible to add them. The second issue is that all these error criteria have different scales. For example, positions have very big values compared to velocities and accelerations. This means then that positions will have much bigger error values with respect to the other variables, when the error percentage might not necessarily be that big compared to these variables. This then means that when all errors are added, the position error will have a huge contribution in the total error when this should not necessarily be the case. The normalized errors will be added because after all errors are given the same scale, adding them up gives a good representation of the total error.

To solve these two issues, each error criterion value will be normalized. This way, all errors become dimensionless. The normalization method that is chosen is to divide the error value by the mean of the measured signal for the specific variable that is used. This can be seen for the position error as an example in (2.19). This normalization method is done for the position, velocity and acceleration errors. The angular errors are normalized using the same method, but with a small difference. The difference is that the normalization factor is taken to be the mean of the absolute value of the measured variable. The absolute value is taken because the angular variables can have negative values. This can cause the total normalized error to be negative and even if it does not end up being negative, it will be skewed down generally. The position, velocity and acceleration can be negative as well, however for all the measurements that were conducted this is not the case.

$$\epsilon_{p_{nor}} = \frac{\epsilon_p}{\bar{p}_{measured}} \tag{2.19}$$

Where $\epsilon_{p_{nor}}$ is the normalized position error and $\bar{p}_{measured}$ is the normalization factor, which is the mean of the measured position.

The error of each variable as well as the normalized error have been computed. In addition to this, all the normalized errors have been added up to obtain the total error within the dataset. This can be seen in Table 2.1.

Table 2.1: Errors and normalized errors for all variables

	ϵ_p	ϵ_v	ϵ_a	ϵ_{γ_1}	ϵ_{ψ_1}	ϵ_{ψ_2}	$\epsilon_{\dot{\gamma}_1}$	$\epsilon_{\dot{\psi}_1}$	$\epsilon_{\dot{\psi}_2}$	ϵ_{total}
Error Value	0.8942	0.0871	0.0295	0.1070	0.1692	0.0622	0.0043	0.0055	0.0047	-
Normalized error	0.0339	0.0659	0.1528	0.2021	0.0356	0.0142	0.2609	0.0455	0.0391	0.8500

One thing to note from these errors is that the normalized errors of the articulation angle and the articulation angular velocity seem a bit too big compared to the other normalized errors. As a result they increase the total error, which is something that needs to be taken into account when using the total error for other analyses.

3 Forward Driving analysis

In this chapter the forward driving experiments are analyzed. First, checks are made on the measurement data to make sure that all the data is correct and that it makes sense. An animation tool is developed that further allows checking the correctness of the measurement data. Then the loaded and unloaded vehicle configurations are analyzed to see if there are differences between them. After that, the model parameters are tuned to reduce the model error. Finally, the model accuracy is assessed by comparing it to the measurement data.

3.1 Data verification

Usually it is assumed that measured data is reliable and accurate, but this is not always the case. There could be inaccuracies arising from the sensor because it might potentially be faulty, it might have not been calibrated properly or it might have not been connected properly. The sensors measure many signals from the vehicle, they can be seen in the work from the previous BEP student [1]. To verify whether these signals are consistent, all the signals in the model are compared to the measurement data. This is for the already existing signals and for the ones that were discussed in section 2. Verifying the measurement data is important because it is vital to know which signals are not correct and which ones are fine so that comparisons can safely be made using the correct signals and the incorrect ones can be neglected. If a measured signal is not correct, it is important to be able to explain the cause.

Multiple measured signals and even some modeled signals show a significant amount of noise, which makes them really hard to view and analyze. Therefore, they are filtered using a third order Butterworth filter with a sampling frequency of 100 Hz and a cutoff frequency of 1 Hz [1].

The OxTS sensors on the vehicle measure the signals with respect to two frames, the horizontal frame and the vehicle frame. The horizontal frame is a frame that only rotates with the yaw angle of the vehicle, while the vehicle frame rotates with all three rotation angles, the roll angle, pitch angle and yaw angle [1], [3].

From the OxTS sensors, it is found that the acceleration in the horizontal frame is fine; however, the acceleration in the vehicle frame appears to have an offset. This offset is especially visible in the lateral acceleration. This can be seen in Figure 3.1 and Figure 3.2. The plots of the longitudinal acceleration can be seen in Appendix D.

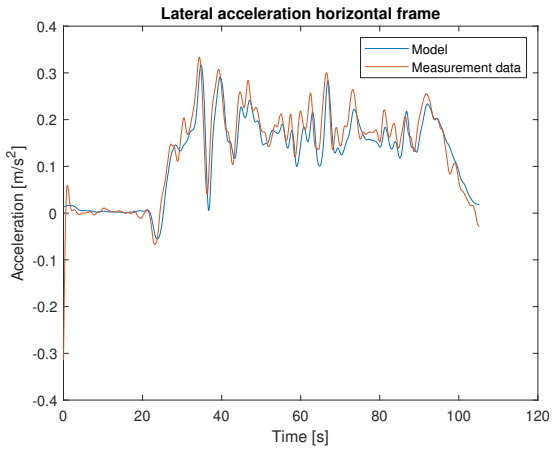

Figure 3.1: Horizontal frame lateral acceleration

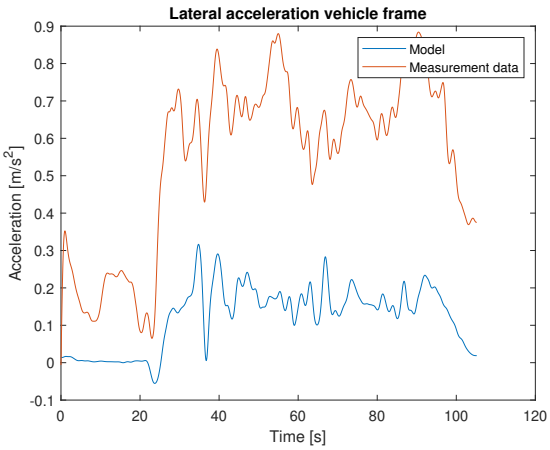

Figure 3.2: Vehicle frame lateral acceleration

This offset requires an explanation. It is caused by how the vehicle frame is defined. The roll rotation of the vehicle combined with gravity cause the vehicle to have an extra acceleration component in the lateral direction. Because as mentioned, the vehicle frame rotates around all three rotation angles, this extra acceleration is included in the total lateral acceleration of the vehicle. In order to actually prove this, this extra acceleration needs to be calculated and removed from the measured lateral acceleration in the vehicle

frame to see whether this will give a similar acceleration to the horizontal frame acceleration and to the model. The corrected lateral acceleration reads

$$a_y = a_{y_{vf}} - \phi g \tag{3.1}$$

where a_y is the corrected lateral acceleration in the vehicle frame, $a_{y_{vf}}$ is the original measured lateral acceleration in the vehicle frame, ϕ is the roll angle and g is the gravitational acceleration constant. Figure 3.3 shows the plot of the contribution of gravity and the roll angle to the lateral acceleration compared to the total lateral acceleration in the vehicle frame. Figure 3.4 shows the new vehicle frame lateral acceleration after removing the gravity and roll angle contribution compared to the horizontal frame lateral acceleration.

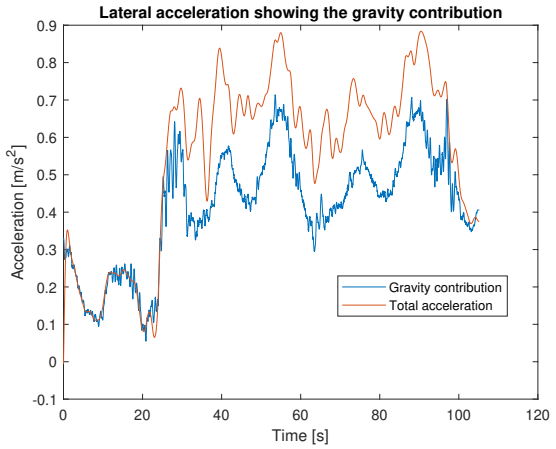

Figure 3.3: Gravity and roll angle acceleration contribution

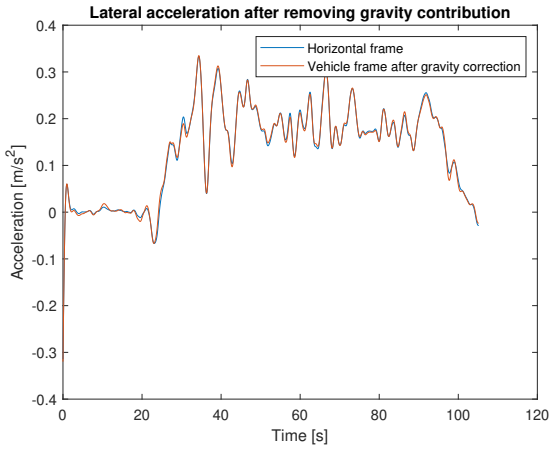

Figure 3.4: New vehicle frame lateral acceleration without the gravity and roll angle acceleration

As can be seen, this gravity contribution is actually quite big and results in a higher lateral acceleration. In Figure 3.4 it can be seen that after removing this contribution, the vehicle frame acceleration becomes almost the same as the horizontal frame acceleration.

The vehicle frame longitudinal acceleration also shows an offset compared to the model and to the horizontal frame longitudinal acceleration. This offset can also be explained by the gravity acceleration. In the longitudinal direction, the pitch angle causes this acceleration. The new vehicle frame longitudinal acceleration is computed by removing the gravity and pitch angle acceleration like it was done for the lateral acceleration in (3.1). The plots for this can be seen in Appendix D. This fixes the vehicle frame longitudinal acceleration and it is now almost exactly the same as the horizontal frame longitudinal acceleration.

The yaw acceleration of both the tractor and the semi-trailer is also found to be incorrect, it appears to have a sign error. This can be seen in Figure 3.5. It is found that when processing the data, a negative sign was included by mistake. Therefore, this has been removed and the yaw acceleration is now considered fine to use and it will be used normally in the rest of the report. The corrected yaw acceleration plot can be seen in Figure 3.6.

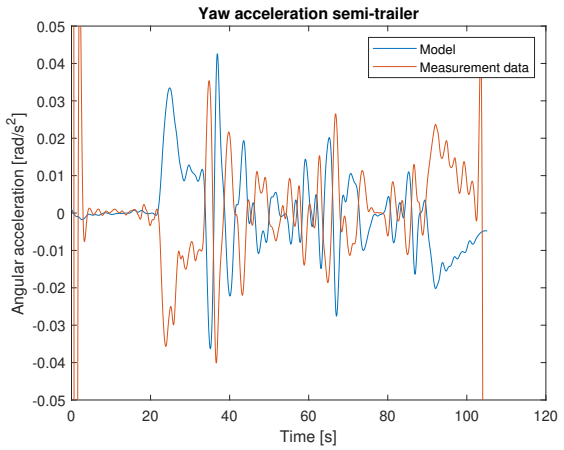

Figure 3.5: Initial tractor Yaw acceleration plot

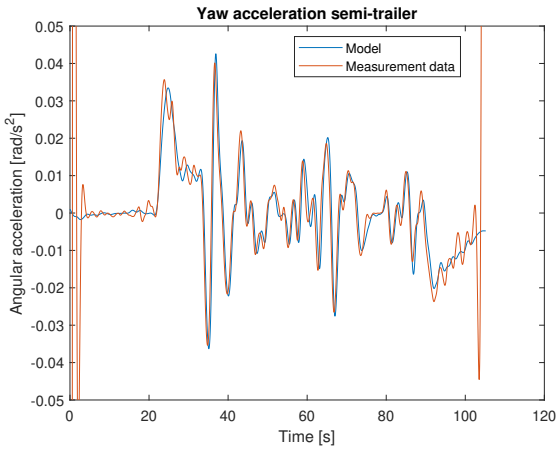

Figure 3.6: Corrected tractor yaw acceleration plot

The last signals that appear to have inaccuracies are the wheel velocities that are measured via the CAN bus. They can be seen in Figure 3.7 and Figure 3.8. These plots show the velocities of the right wheel and the left wheel in the model and the measurement data. They also show the longitudinal velocity of the vehicle to see how it compares to the measured wheel velocities. The wheel velocities in the model have been modeled as transnational velocities. Normally, it is expected that when the vehicle is turning the wheel that has a bigger turning radius has a bigger velocity than the inner wheel. However, the average of both wheel velocities should give the longitudinal velocity of the vehicle. This is the case for the modeled wheel velocities, but not for the measured ones.

An explanation for this could not be found. when the vehicle is driving with a certain velocity, the wheel velocities are just zero, which is completely illogical. The rear axle right wheel appears to have a velocity of 0 throughout the entire measurement. In addition to this, for the wheel velocities at the front axle, it seems like the right wheel and left wheel velocities are flipped. This would mean that one wheel has a velocity in one direction, while the other one has the same velocity but in the reverse direction. Therefore, an explanation could not be found and it is assumed that this is an error from the sensor. The measured wheel velocities will not be considered anymore for the rest of the report.

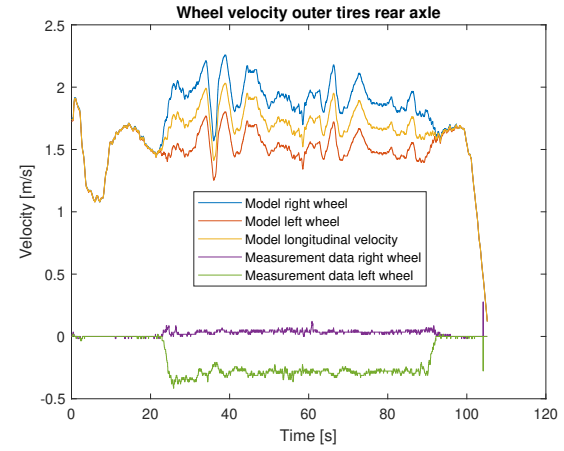

Figure 3.7: Wheel velocity tractor rear axle

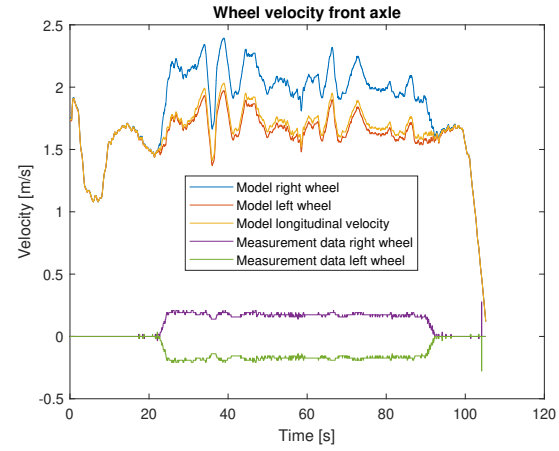

Figure 3.8: Wheel velocity tractor front axle

3.2 Animation tool

In the previous subsection all measured signals have been checked to see if any of them contain errors. The vehicle has two OxTS sensors mounted on it, one on the tractor and one on the semi-trailer [1]. An animation tool that visualizes the measured trajectory that the vehicle has travelled is developed to check whether both sensors judge the distance between them correctly.

This animation tool has four inputs, the positions of the tractor axles, the position of the center semi-trailer axle and the position of the fifth wheel. However, the sensors on the vehicle do not measure the positions at these points [1]. Therefore, the measured sensor positions need to be shifted to all the points on the vehicle that were mentioned. This is done in the same way as in (2.7). Although, instead of shifting the positions at the axles to the sensor positions as was done in this equation, the sensor positions are now shifted to the axle positions as well as the fifth wheel position. Figure 3.9 shows the animation right at the start and Figure 3.10 shows the animation when the vehicle is turning. The animation shown is for a constant steer test.

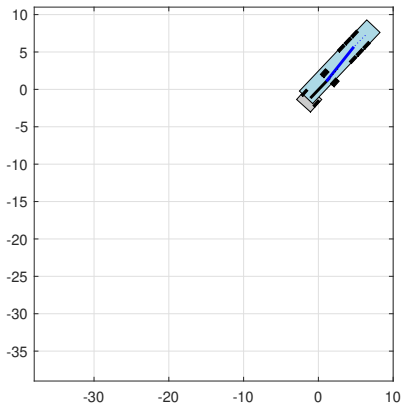

Figure 3.9: Animation at the start

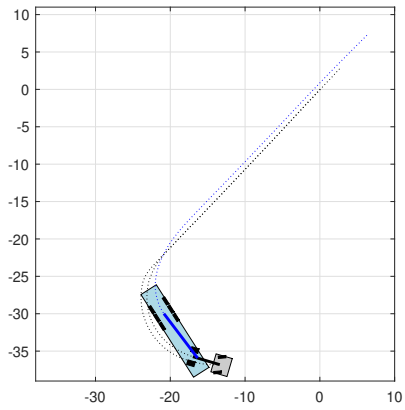

Figure 3.10: Animation during turning

From Figure 3.9 it can be seen that the vehicle pose appears to be wrong at the start. The observation is that the tractor and the semi-trailer appear to be going into each other, which should not be the case. This implies that in the measurement data when both the tractor and the semi-trailer are each assumed to be separate bodies, they do not align together like they should. The main observation here is that the sensors appear to not calculate the distance between them properly because the tractor and semi-trailer are going into each other like mentioned.

Later on in the animation in Figure 3.10, the vehicle pose starts to turn. In this case, the vehicle starts to look more feasible than before. However, the fifth wheel appears to be shifted slightly to the left. Generally, the visual state of the vehicle is always changing. Sometimes it looks completely incorrect as in Figure 3.9 and at other times it looks slightly better as in Figure 3.10. It ranges between these two states throughout the whole animation.

The fact that the distance between the tractor and the semi-trailer keeps changing may indicate some accuracy problems with the OxTS system. To check this, both sensor positions will be shifted to the position of the fifth wheel. This is because the fifth wheel is the only common point on the vehicle for the tractor and the semi-trailer. Then the difference between both shifted positions will be found. This will give an indication of whether the OxTS sensors actually judge the distance between them incorrectly. This is done in the global frame. Figure 3.11 and Figure 3.12 show the resulting plots of taking this difference for the longitudinal direction and the lateral direction respectively.

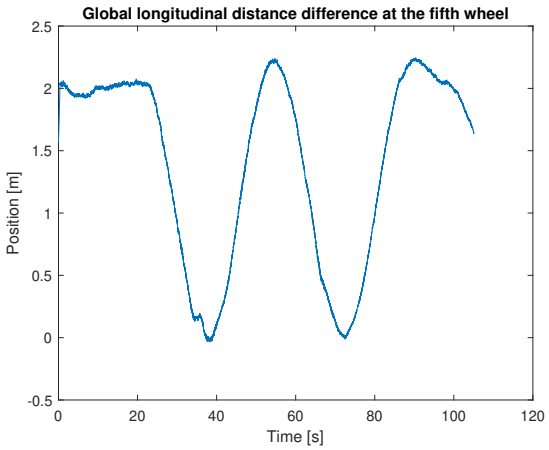

Figure 3.11: Global longitudinal difference

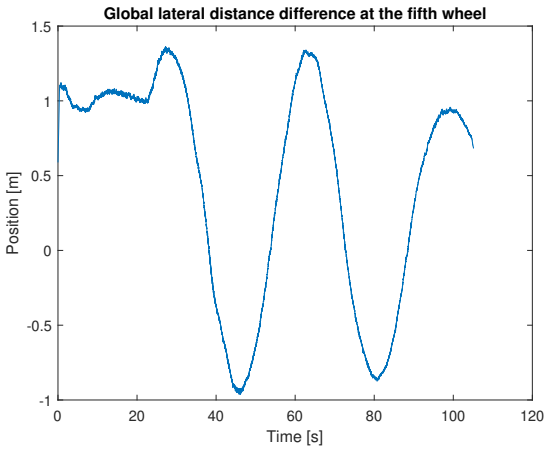

Figure 3.12: Global lateral difference

From the plots, it can be observed that the difference in distance at the fifth wheel does appear to be changing.

3.3 Loaded and unloaded vehicle configurations

As mentioned in section 1, some measurements were made with the vehicle being loaded and some with the vehicle being unloaded. The load that was used is $12,000\ kg$ [1]. The goal is to analyze whether this load causes a different behavior or not. More precisely, analyze whether it has an effect on the model accuracy. The model is a kinematic model, which means that it does not model any masses or forces.

There are three left constant steer tests that were conducted with the same maneuver with the only difference being that some are loaded and some are unloaded. Therefore, they are identical in every aspect apart from being loaded or unloaded. These measurements are going to be compared to the model to see which condition the model represents more accurately.

In subsection 2.4, the position, velocity and acceleration error criteria are defined for the semi-trailer. However, in this comparison the same error criteria are also used for the tractor because it is of interest to see whether the added load affects the tractor or the semi-trailer more. The error comparison tables are split into four. The first section is for the tractor errors, the second is for the semi-trailer errors, the third is for the articulation errors and the last is for the total error. Table 3.1 shows the average error of the datasets that were mentioned earlier for the loaded and the unloaded cases. The green highlighted cells represent a smaller error compared to the other configuration. The error comparison of loaded and unloaded configurations for each individual dataset can be seen in Appendix E

Table 3.1: Loaded and unloaded configurations comparison

Tractor	ϵ_{p_1}	ϵ_{v_1}	ϵ_{a_1}	ϵ_{ψ_1}	$\epsilon_{\dot{\psi}_1}$	ϵ_{total_1}
Loaded	1.5592	0.0046	0.0111	0.1295	0.0039	0.1939
Unloaded	1.7005	0.0042	0.0124	0.1281	0.0043	0.2061

Semi-trailer	ϵ_{p_2}	ϵ_{v_2}	ϵ_{a_2}	ϵ_{ψ_2}	$\epsilon_{\dot{\psi}_2}$	ϵ_{total_2}
Loaded	1.2876	0.0283	0.0102	0.1176	0.0022	0.1925
Unloaded	1.6286	0.0312	0.0163	0.1370	0.0029	0.2486

Articulation	ϵ_{γ_1}	$\epsilon_{\dot{\gamma}_1}$	ϵ_{total_γ}
Loaded	0.0300	0.0016	0.3170
Unloaded	0.0400	0.0020	0.3667

Overall	ϵ_{total}
Loaded	0.7034
Unloaded	0.8214

From Table 3.1, it becomes clear that the model represents the loaded case more accurately than the unloaded

case. This is especially the case for the semi-trailer, as in all comparisons, the loaded case has less error than the unloaded case. The loaded case appears to also have less error than the unloaded case for the tractor, however the difference is small.

The conclusion is that the model represents the loaded cases more accurately than the unloaded cases. The loaded measurements have a smaller error, especially for the semi-trailer. For the tractor, the loaded cases appear to be only slightly better represented by the model.

It is important to understand why the model represents the loaded cases better than the unloaded ones. The load seems to affect the semi-trailer more than it affects the tractor. This can be explained by the fact that the load is put inside the semi-trailer, so the semi-trailer receives more of this load than the tractor does. Normally, the semi-trailer turns about its center axle. This means that the wheelbase of the semi-trailer is the distance from the fifth wheel to the center axle of the semi-trailer. However, when the semi-trailer is loaded, it might be that this rotation point changes to the first axle of the semi-trailer. This then gives a shorter wheelbase. In order to verify whether this is the case or not, the wheelbase of the semi-trailer l_2 is varied for both the loaded and the unloaded cases separately, until values for l_2 are found for the loaded case and for the unloaded case for which their error values are really similar. This will only include the original error criteria that were formulated in subsection 2.4, so the position, velocity and acceleration error criteria of the tractor will not be included. This is because of the fact that these signals are not dependent on l_2, therefore when l_2 is varied this error will remain the same.

The original length of l_2 is 8.15 m. The distance between the center semi-trailer axle and the first semi-trailer axle is 1.31 m. This then means that l_2 would become 6.84 m for the loaded cases, while for unloaded cases it would stay around the same if the theory for what has been discussed is true.

It is found that there are three l_2 combinations for the loaded and unloaded cases that give the least error difference between both cases. This error difference is in the order of 10^{-4}. Table 3.2 shows the error difference between loaded configurations and unloaded configurations of the average total error for both configurations.

Table 3.2: Error difference between loaded and unloaded configurations for different l_2 combinations

	Error difference	**Total error**	l_2 **loaded [m]**	l_2 **unloaded [m]**
Combination 1	$4.70 \cdot 10^{-4}$	0.5923	7.2	7.9
Combination 2	$7.63 \cdot 10^{-4}$	0.5680	8.2	7.8
Combination 3	$7.69 \cdot 10^{-4}$	0.7034	6.9	8.2

From the results, it can be seen that combinations 1 and 3 support the claim, especially combination 3. For combination 1, the lengths l_2 for the loaded and unloaded cases are almost as predicted; however, they are slightly bigger and slightly smaller for loaded and unloaded cases respectively. Combination 3 however supports this claim perfectly, as l_2 becomes just like predicted earlier for both loaded and unloaded configurations. On the other hand, combination 2 does not support the claim at all.

To conclude this analysis, it seems that the claim that was made earlier appears to be supported by the results. However, combination 3, which is the one that supports the claim the most has the most error out of all combinations. Combination 1 has the least error and it is the combination that does not support the claim. Therefore, it would not be a valid conclusion to conclude that the load causes the wheelbase of the semi-trailer to change. This is something that could be better validated in future research. Also another effect that might be causing the differences between loaded and unloaded cases is side slip of the axles. As mentioned in subsection 2.1, the model neglects side slip. However, this is something that is outside the scope of this research and will be left for future research.

3.4 Tuning the steering system parameters

The parameters of the steering system that are shown in (2.13) will be tuned and optimized. Having the optimized parameters is crucial because the best performance of the model is desired when comparing it to the measurement data. The measurement data is split into two sets, a training set and a validation set.

This is done to avoid over fitting the model to the measurement data. The optimum parameters are found through the training set and they are tested on the validation set. Table 3.3 shows the baseline values of the parameters.

Table 3.3: Original parameters

Parameter	Value
i_{steer}	22
a_2	0

Since both of these parameters are related, they both need to be changed simultaneously, until the optimum values are found. Figure 3.13 shows a heatmap of the effect of changing both i_{steer} and a on the average total error of the used measurements.

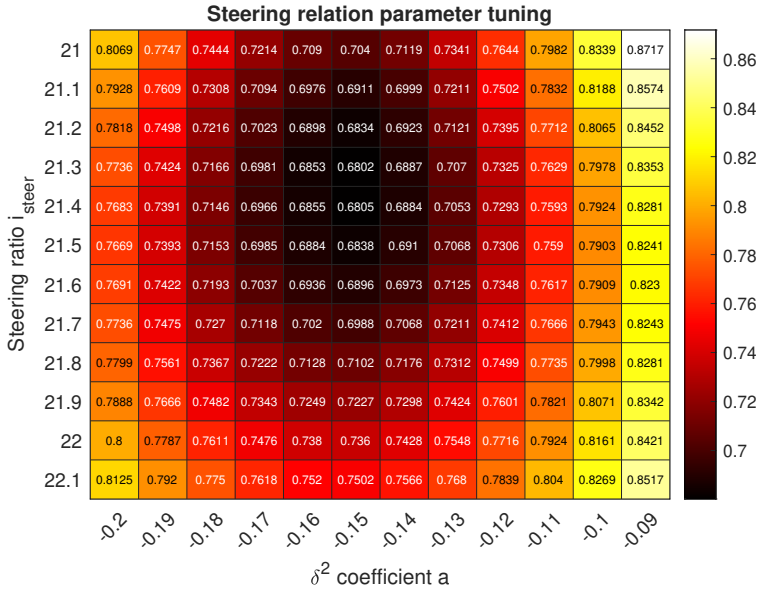

Figure 3.13: Heatmap for parameter optimization

From this heatmap, it becomes clear that the smallest error occurs for $i_{steer} = 21.3$ and $a = -0.15$, which means that these are the optimum values for these parameters. The negative value of a is quite logical because as discussed in subsection 2.3, the inner front wheel always has a bigger steering angle than the outer front wheel.

In order to verify that these parameters improve the model accuracy, they are tested on the validation set. Table 3.4 shows a comparison of the average total error with the original parameters and the optimized parameters.

Table 3.4: Optimized parameters validation

	CS$_L$	**CS$_R$**	**TR1**	**TR2**	**fig8**	**Total**
Baseline parameters	0.6977	0.9686	1.5849	0.8857	1.4227	1.1119
Optimized parameters	0.6790	0.8660	0.9019	0.6257	0.5627	0.7271

From this table, it can be concluded that the optimized steering system parameters do indeed reduce the total error of the model.

3.5 Assessing the model accuracy

Comparisons between the model and the measurement data can be made to evaluate the accuracy of the model. The comparisons are made by usual inspection of plots and also by using the error criteria that were defined in subsection 2.4. The baseline model is the initial model that was made. The optimized model is the model that uses the optimized parameters that were determined in subsection 3.4. It would be redundant to compare the baseline model to the measurement data and then also compare the model after it has been optimized to the measurement data. Therefore, the comparisons with the measurement data are made using the optimized model only.

Model comparison to measurement data has been done before, mainly for positions and angular velocities [1]. Therefore, this comparison will mostly be done with the new signals that were formulated in subsection 2.2, but if necessary the existing signals will be analyzed as well. Table 3.5 shows the average error for all experiments. The green highlighting indicates the experiment type that has the smallest error, while a red highlighting indicates the experiment type that has the largest error.

There are four new signals that need to be compared to the measurement data, they are the global velocity, the local velocity, the acceleration and the angular acceleration. In Appendix F, for each of these signals plots are shown for the measurement that gives the most error and for the measurement that gives an error that is closest to the average error for each of these signals.

Table 3.5: Average error for each dataset for all errors

	CS$_L$	**CS$_R$**	**TR1**	**TR2**	**fig8**	**Total**
ϵ_p	1.3363	2.0745	2.2403	0.9920	2.0905	1.7467
ϵ_v	0.0418	0.0773	0.0532	0.0164	0.0334	0.0444
ϵ_a	0.0187	0.0377	0.0256	0.0154	0.0154	0.0226
ϵ_{γ_1}	0.0402	0.0729	0.0673	0.0198	0.0225	0.0445
ϵ_{ψ_1}	0.1092	0.1486	0.1733	0.2291	0.1309	0.1582
ϵ_{ψ_2}	0.1154	0.1848	0.1368	0.2149	0.1328	0.1569
$\epsilon_{\dot{\gamma}_1}$	0.0022	0.0045	0.0108	0.0032	0.0045	0.0051
$\epsilon_{\dot{\psi}_1}$	0.0045	0.0057	0.0121	0.0054	0.0059	0.0067
$\epsilon_{\dot{\psi}_2}$	0.0031	0.0044	0.0043	0.0037	0.0040	0.0039
ϵ_{total}	0.6230	0.8116	0.8632	0.6970	0.5055	0.7001

From the table it can be seen that the model accurately represents left constant steer tests, the transient response 2 tests and the figure8 tests. The right constant steer tests and the transient response 1 tests are still well represented by the model, but not as good as for the other tests. It should be noted however that not all experiments have the same number of measurements, so this might not give the most accurate representation of the errors for all the experiments.

Overall, the model appears to give a good representation of the measurement data. One thing that the model could be lacking in is the fact that it does not accurately represent all the experiments, as seen in Table 3.5. Therefore, future research could be to investigate how to make all the errors from all experiments more equal.

4 Reverse Driving Analysis

In this chapter, reverse driving of the vehicle is analyzed. First, it is analyzed with the baseline model. Then a controller is developed that stabilizes the vehicle and improves the tracking performance. Finally, this controller is tuned to obtain the most accurate results and they are compared to the measurement data.

4.1 Reverse driving stability

It is known that a tractor semi-trailer vehicle is unstable when driving backwards. Unstable means that while driving backwards, when a small steering angle is applied, the articulation angle between the tractor and the semi-trailer keeps growing exponentially until the vehicle is about to jackknife. Therefore, it is difficult for drivers to reverse [4]. In the model, the articulation angle also keeps growing very quickly. This not only causes the vehicle to jackknife, but also not follow the desired path. Figure 4.1 shows an illustration of this for a step steer test, while Figure 4.2 shows how the modeled articulation angle keeps increasing. In addition to this, all the errors of the model also become very high when reversing, This can be seen in Table 4.1

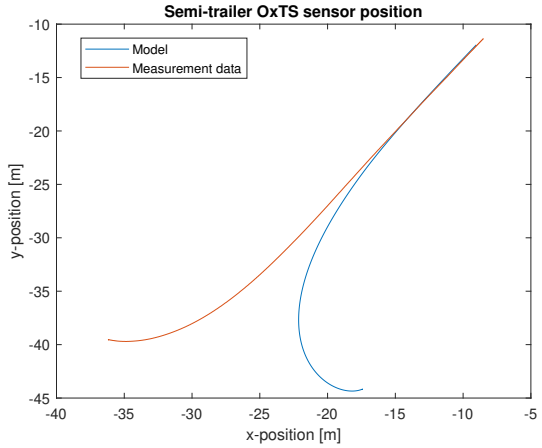

Figure 4.1: Reverse driving modeled path compared to measured path

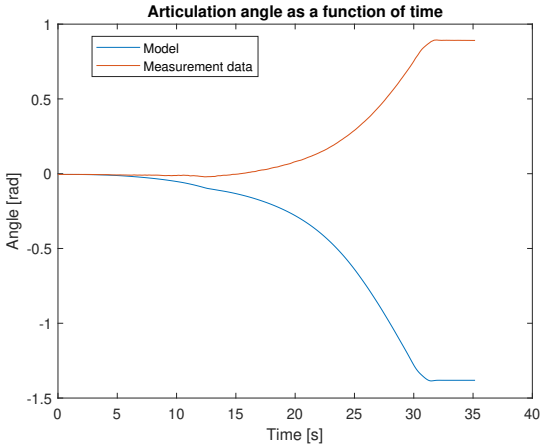

Figure 4.2: Reverse driving modeled articulation angle compared to measured articulation angle

Table 4.1: Error values for a reverse driving step steer test

	ϵ_p	ϵ_v	ϵ_a	ϵ_{γ_1}	ϵ_{ψ_1}	ϵ_{ψ_2}	$\epsilon_{\dot{\gamma}_1}$	$\epsilon_{\dot{\psi}_1}$	$\epsilon_{\dot{\psi}_2}$	ϵ_{total}
Error value	2.0764	0.1089	0.0599	0.6672	0.0279	0.6393	0.0648	0.0034	0.0636	9.4526

4.2 Reverse driving controller

When a small steering angle is applied on the vehicle, the articulation angle increases exponentially. This causes the semi-trailer to follow a different path than the one it should have followed. This then also causes all the other errors for the velocity and acceleration to become much higher.

The aim is to stabilize the vehicle combination. This is done using a proportional controller. The idea of this controller is that when the articulation angle starts to become bigger than it should be, the controller feeds the increase of the articulation angle into the steering input of the model so that the front wheel angle is adjusted to reduce the articulation angle. This is demonstrated in the control scheme in Figure 4.3 in (4.1). This way the articulation angle never becomes too big and so the vehicle remains stable, the desired path is followed and the errors decrease.

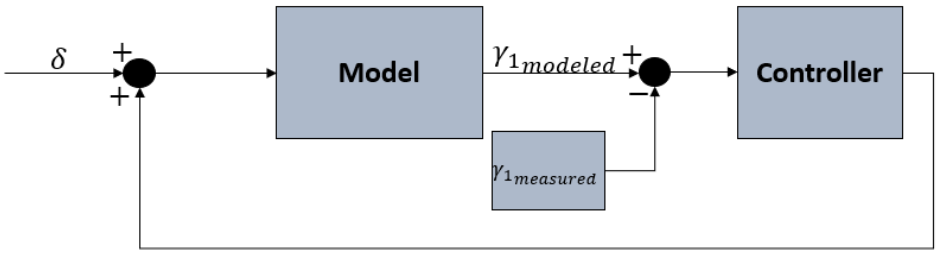

Figure 4.3: Control scheme of reverse driving

$$\delta = \delta + K(\gamma_{1_{modeled}} - \gamma_{1_{measured}}) \tag{4.1}$$

K is the gain of the controller and it needs to be tuned. The controller is demonstrated in the Simulink model, which can be seen in Appendix G. In the Simulink model, the desired articulation angle is the measured articulation angle that is taken from the measurement data. The difference between the modeled and the measured articulation angles is found and is fed into the controller. The controller multiplies this difference with its gain and the needed steering adjustment is obtained. This steering adjustment is added to the input steering angle, so that the total steering input is obtained. The total steering input is fed into a switch. This switch selects which steering input to use, whether it is the original one or the adjusted one, which has just been described. The switch makes that decision based on a condition. The condition here is that if the vehicle is driving forward, then it should use the original steering input. If the vehicle is driving backwards, then it should use the adjusted steering input. The controller is initially tested with a gain of 1. The results of the same step steer test that was shown in Figure 4.1 and Figure 4.2 can be seen in Figure 4.4 and Figure 4.5. The errors can be seen in Table 4.2.

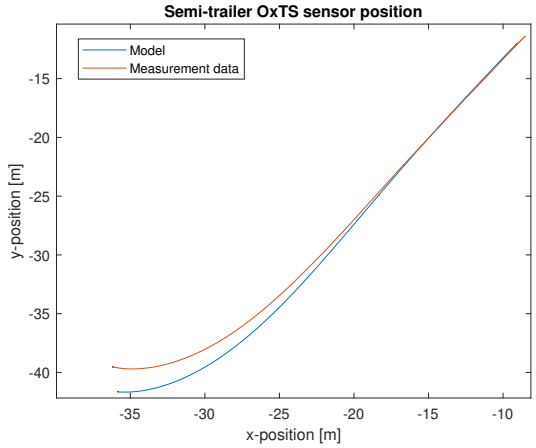

Figure 4.4: Position with the controller

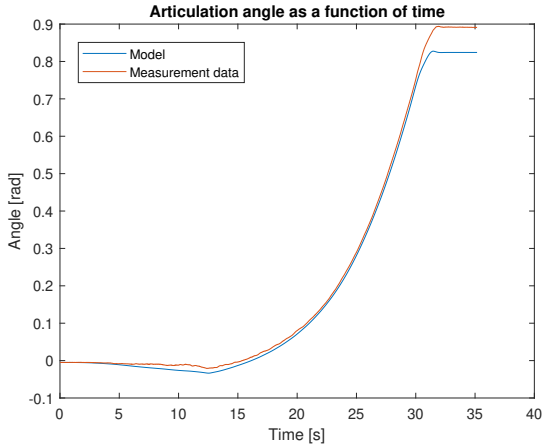

Figure 4.5: Articulation angle with the controller

Table 4.2: Error values for a step steer test with the controller

	ϵ_p	ϵ_v	ϵ_a	ϵ_{γ_1}	ϵ_{ψ_1}	ϵ_{ψ_2}	$\epsilon_{\dot{\gamma}_1}$	$\epsilon_{\dot{\psi}_1}$	$\epsilon_{\dot{\psi}_2}$	ϵ_{total}
Error value	1.3763	0.0402	0.0256	0.0161	0.0271	0.0425	0.0027	0.0041	0.0041	1.2466

As can be observed there is significant improvement for the position error. In addition to this, the articulation angle is now stabilized and is similar to the measured one. Furthermore, the error has gone down significantly for every single variable.

It is of interest to know how much the steering angle is adjusted by the controller. It is possible to see that by looking at the plot for the original steering input compared to the adjusted steering angle. This can be seen in Figure 4.6.

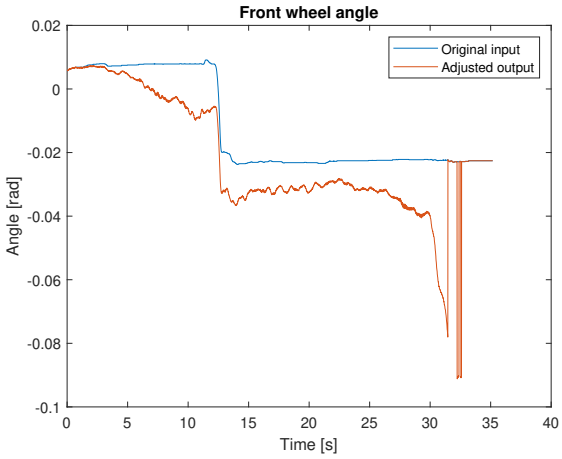

Figure 4.6: Original steering angle input compared with adjusted steering angle output

From the plot, it is clear that the controller is doing quite a lot of adjustment to the steering angle. It is good that the controller stabilizes the articulation angle with these adjustments, however this also means that the model is not that great for reverse driving because of the large adjustments that need to be made to stabilize the vehicle.

4.3 Tuning the controller

The final step is tuning the controller and optimizing the gain in order to obtain the best performance. This is done in the same way as in subsection 3.4, in the sense that the measurements are split into two sets, a tuning set and a validation set to not over fit the model. For tuning the gain, the most important error criterion to look at is the position. This is because of two reasons. The first reason is that the main goal of stabilizing reverse driving is to make sure that the model follows the measured path better. The other reason is that when the gain is increased most errors decrease, whereas for the position error this is not always the case. Therefore, the optimum gain needs to be found for which the position error is as close as possible to the minimum.

The optimum gain is found to be 5. Table 4.3 shows the original and optimized average error of the position error and the total error for each experiment type, where the baseline case is with a gain of one. The total error however does not include the articulation angle error and the articulation angular velocity error. This is because as mentioned in subsection 2.5, they increase the total error too much. In this case when the gain of the controller is increased, the articulation error will constantly keep decreasing. This means that the total error will show a large decrease, which might give a misleading representation of the total error because the other errors might have not decreased by that much. Instead, the articulation error is analyzed separately.

Table 4.3: Comparison between the errors with the tuned gain and the errors with the original gain

	D1	**D2**	**D3**	**D4**	**SSR**$_L$	**SSR**$_R$	**Total**
Original ϵ_p	1.8402	1.1915	2.7980	1.6008	3.3897	1.3488	2.0282
Original $\epsilon_{\gamma_1+\dot{\gamma}_1}$	0.2855	0.2504	0.4098	0.2615	0.4957	0.1854	0.3147
Original ϵ_{total}	0.8693	0.5642	1.0748	0.5751	2.4222	1.0570	1.0938
Optimized ϵ_p	1.6574	1.0482	2.8932	1.6986	3.4845	1.3290	2.0185
Optimized $\epsilon_{\gamma_1+\dot{\gamma}_1}$	0.2477	0.2099	0.2860	0.2425	0.4076	0.1339	0.2546
Optimized ϵ_{total}	0.8519	0.5524	0.9721	0.5873	2.3081	1.0608	1.0554

From the table it can be seen that having a gain of 5 has a small, but mostly positive effect on the errors. However, the reduction in errors is not that big, but this is because of the fact that having a gain of 1 already improves reverse driving significantly.

5 Conclusion & Recommendations

5.1 Conclusion

In this research, a tractor semi-trailer kinematic vehicle model has been analyzed, extended and improved. A contribution is the new equations that provide the velocity and acceleration of the kinematic model

It is found that the vehicle frame acceleration needs the removal of the gravity and roll angle acceleration contribution to make it match with the model. During processing of the measurement data, the yaw acceleration appears to have an incorrect negative sign. Lastly, it has been found that the measured wheel velocities do not make much sense at all.

Using the animation tool that has been developed it is found that the sensors have a limited accuracy. This causes the tractor and the semi-trailer in the animation tool to appear as if they were on top of one another.

It is found that loaded measurements are better represented by the kinematic model than unloaded measurements, especially for the semi-trailer. However, this does not disqualify the unloaded measurements, as they are still deemed to be accurate enough. It is also found that it is possible to obtain similar errors for both configurations by adjusting the wheelbase of the semi-trailer.

An expression is defined that models the asymmetric steering system using a quadratic polynomial, instead of the Ackermann steering relations. The parameters in this expression were tuned and optimized. The most important finding though is the fact the coefficient of δ_h^2, a was negative. This gives an indication that the steering behavior is non linear and in order to get the best representation, a negative coefficient is needed.

In reverse driving the vehicle is unstable. However, the vehicle can be stabilized using a controller. It is demonstrated that this controller is very effective in stabilizing the vehicle and improving the model's path following performance. Despite this, the heavy dependence on the controller indicates that the model is not great for reverse driving. Furthermore, the gain of the controller has been tuned and optimized.

5.2 Recommendations

The error criteria that are defined for the position, velocity and acceleration do not always give the most accurate results. This is because they are defined using the difference in the modeled and the measured magnitude. However, there can be two points at completely different coordinates that have the same magnitude. If that is the case, the error would be 0, which is incorrect. Therefore, better and more reliable error criteria need to be defined for these signals.

The articulation angle and the articulation angular velocity error criteria can also be a bit misleading. This is due to the fact that the articulation angle is calculated by subtracting the yaw angles ψ_2 from ψ_1. This means that there might be errors in both ψ_1 and ψ_2 that get cancelled out.

The error normalization method that has been used does not always give the same weighting for all the errors. This is observed for the articulation angle error and the articulation angular velocity error, as their normalized error values are almost always much larger than the other normalized errors. Therefore, they increase the total error. Because of that, a better error normalization method should be found.

The current animation tool that is being used shows that the tractor and semi-trailer sensors appear to incorrectly judge the distance between them. Further investigations need to be made about the sensor's accuracy.

It has been found that by adjusting the semi-trailer wheelbase, it was possible to match the loaded configuration errors with the unloaded configuration errors. However, this could also be due to the fact that the load causes side slip on the vehicle's axles. This has not been investigated as it is outside the scope of this research, however it is something that can be done in future research.

The model represents the measurement data quite well, but it does not represent all experiments with the same accuracy. For consistency, it would be desired for that to be the case. This is something that could be looked into for future research.

A controller has been developed that stabilizes reverse driving. However, a controller should also be developed for forward driving that improves the path tracking performance of the model.

References

[1] S. ter Braake, "Accuracy evaluation of a kinematic tractor semi-trailer model using real-world measurement data dc 2022.014," 2022.

[2] I. Besselink, "Vehicle dynamics-4at000 lecture notes," 2021.

[3] O. T. Solutions, "User manual covers rt3000 v3 and rt500 v1 models the inertial experts. rt gnss-aided inertial measurement systems," 2020. [Online]. Available: http://www.oxts.com

[4] Z. Leng and M. Minor, "A simple tractor-trailer backing control law for path following," *IEEE/RSJ 2010 International Conference on Intelligent Robots and Systems, IROS 2010 - Conference Proceedings*, pp. 5538–5542, 2010.

Appendices

A Semi-trailer Equations

The semi-trailer OxTS sensor position is given by

$$\begin{bmatrix} x_{2_{OxTS}} & y_{2_{OxTS}} \end{bmatrix} = \begin{bmatrix} x_2 & y_2 \end{bmatrix} + \begin{bmatrix} l_{x2} & l_{y2} \end{bmatrix} \begin{bmatrix} -\cos(\psi_2) & -\sin(\psi_2) \\ \sin(\psi_2) & -\cos(\psi_2) \end{bmatrix} \tag{A.1}$$

The semi-trailer global velocity at the OxTS sensor location is given by

$$\begin{bmatrix} \dot{x}_{2_{OxTS}} & \dot{y}_{2_{OxTS}} \end{bmatrix} = \begin{bmatrix} \dot{x}_2 & \dot{y}_2 \end{bmatrix} + \begin{bmatrix} l_{x2} & l_{y2} \end{bmatrix} \begin{bmatrix} \sin(\psi_2)\dot{\psi}_2 & -\cos(\psi_2)\dot{\psi}_2 \\ \cos(\psi_2)\dot{\psi}_2 & \sin(\psi_2)\dot{\psi}_2 \end{bmatrix} \tag{A.2}$$

The semi-trailer local velocity at the OxTS sensor location is given by

$$\begin{bmatrix} V_{x2_{OxTS}} & V_{y2_{OxTS}} \end{bmatrix} = \begin{bmatrix} \dot{x}_{2_{OxTS}} & \dot{y}_{2_{OxTS}} \end{bmatrix} \begin{bmatrix} \cos(\psi_2) & -\sin(\psi_2) \\ \sin(\psi_2) & \cos(\psi_2) \end{bmatrix} \tag{A.3}$$

Lastly, the semi-trailer acceleration at the OxTS sensor is given by

$$\begin{bmatrix} a_{x2_{OxTS}} & a_{y2_{OxTS}} \end{bmatrix} = \begin{bmatrix} \dot{V}_{x2_{OxTS}} & \dot{V}_{y2_{OxTS}} \end{bmatrix} + \begin{bmatrix} -V_{y2_{OxTS}} & V_{x2_{OxTS}} \end{bmatrix} \dot{\psi}_2 \tag{A.4}$$

B Acceleration contribution

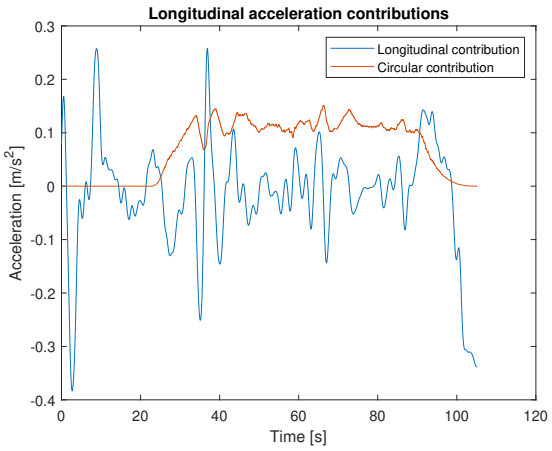

Figure B.1: Acceleration contributions to longitudinal acceleration

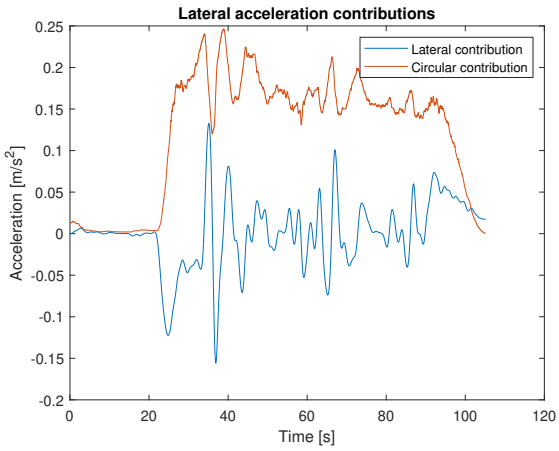

Figure B.2: Acceleration contributions to lateral acceleration

C Error Criteria Extra Plots

Velocity Plots

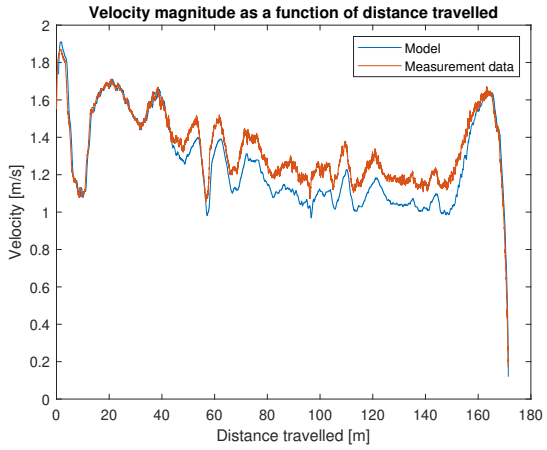

Figure C.1: Velocity Magnitude

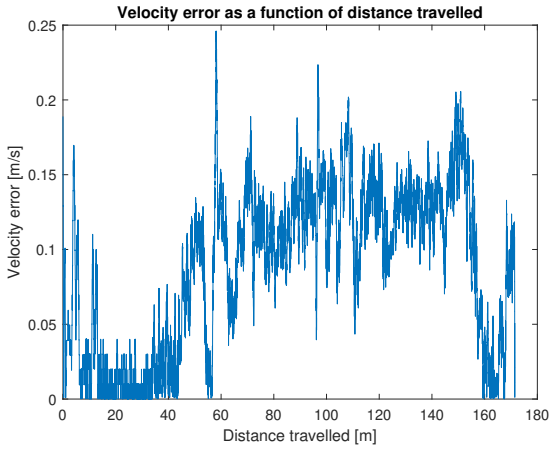

Figure C.2: Magnitude of velocity error

Acceleration Plots

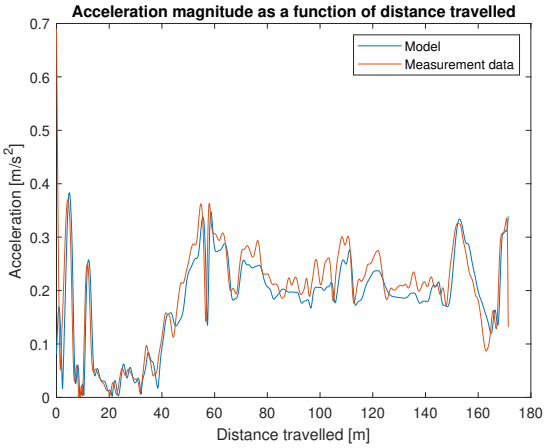

Figure C.3: Acceleration Magnitude

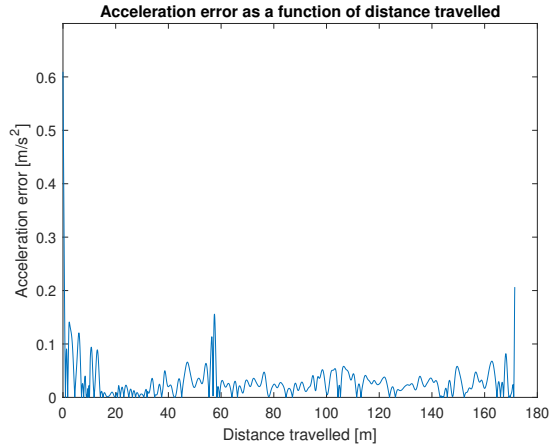

Figure C.4: Magnitude of acceleration error

D Verifying Measurement Data Extra Plots

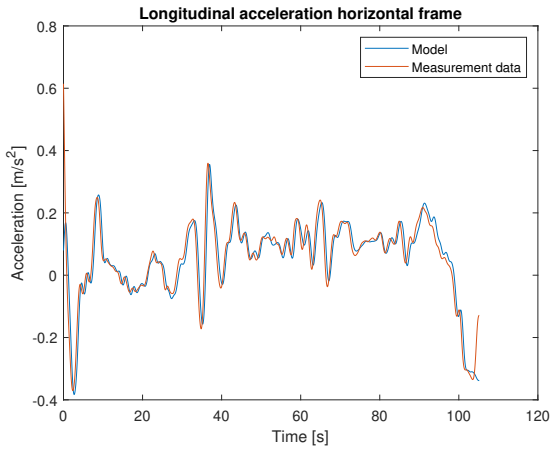

Figure D.1: Longitudinal acceleration in the horizontal frame

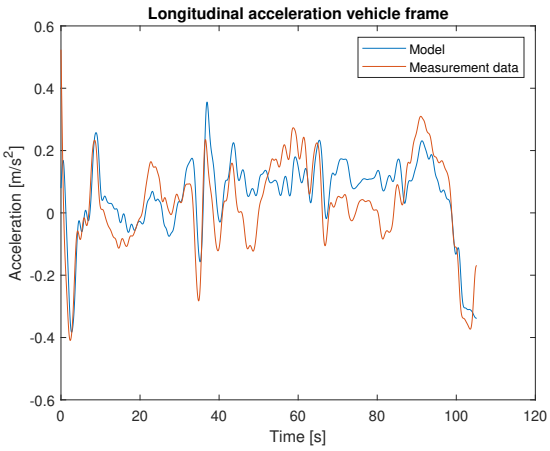

Figure D.2: Longitudinal acceleration in the vehicle frame

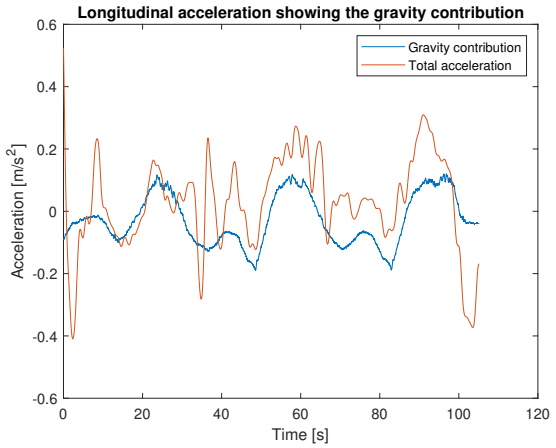

Figure D.3: Gravity and pitch angle acceleration contribution

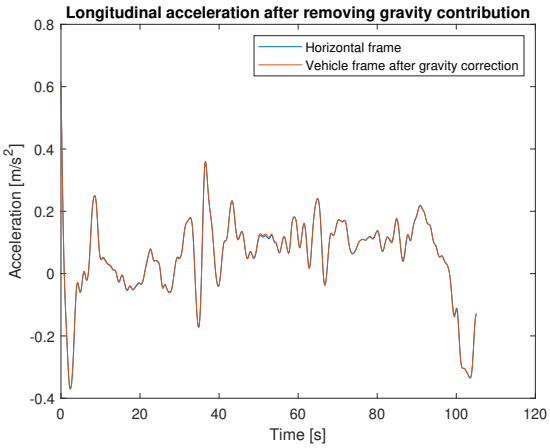

Figure D.4: New vehicle frame longitudinal acceleration

E Loaded and Unloaded Vehicle Configurations Comparisons

Table E.1: CS_L_200s_5v dataset loaded and unloaded configurations comparison

Tractor	ϵ_{p_1}	ϵ_{v_1}	ϵ_{a_1}	ϵ_{ψ_1}	$\epsilon_{\dot{\psi}_1}$	ϵ_{total_1}
Loaded	2.0645	0.0039	0.0091	0.1650	0.0035	0.2199
Unloaded	2.5996	0.0033	0.0094	0.1854	0.0036	0.2530

Semi-trailer	ϵ_{p_2}	ϵ_{v_2}	ϵ_{a_2}	ϵ_{ψ_2}	$\epsilon_{\dot{\psi}_2}$	ϵ_{total_2}
Loaded	1.4383	0.0195	0.0086	0.1272	0.0015	0.1834
Unloaded	2.0925	0.0189	0.0094	0.1643	0.0017	0.2265

Articulation	ϵ_{γ_1}	$\epsilon_{\dot{\gamma}_1}$	ϵ_{total_γ}
Loaded	0.0378	0.0013	0.4321
Unloaded	0.0212	0.0013	0.4097

Overall	ϵ_{total}
Loaded	0.8354
Unloaded	0.8892

Table E.2: CS_L_360s_5v dataset loaded and unloaded configurations comparison

Tractor	ϵ_{p_1}	ϵ_{v_1}	ϵ_{a_1}	ϵ_{ψ_1}	$\epsilon_{\dot{\psi}_1}$	ϵ_{total_1}
Loaded	1.0989	0.0046	0.0145	0.0758	0.0038	0.1757
Unloaded	0.9404	0.0045	0.0149	0.0771	0.0047	0.1772

Semi-trailer	ϵ_{p_2}	ϵ_{v_2}	ϵ_{a_2}	ϵ_{ψ_2}	$\epsilon_{\dot{\psi}_2}$	ϵ_{total_2}
Loaded	1.1054	0.0261	0.0092	0.0773	0.0022	0.1569
Unloaded	1.2185	0.0291	0.0190	0.1081	0.0031	0.2444

Articulation	ϵ_{γ_1}	$\epsilon_{\dot{\gamma}_1}$	ϵ_{total_γ}
Loaded	0.0119	0.0013	0.1693
Unloaded	0.0461	0.0021	0.3293

Overall	ϵ_{total}
Loaded	0.5019
Unloaded	0.7509

Table E.3: CS_L_500s_5v dataset loaded and unloaded configurations comparison

Tractor	ϵ_{p_1}	ϵ_{v_1}	ϵ_{a_1}	ϵ_{ψ_1}	$\epsilon_{\dot{\psi}_1}$	ϵ_{total_1}
Loaded	1.0091	0.0059	0.0118	0.1123	0.0046	0.1600
Unloaded	0.6624	0.0058	0.0157	0.0645	0.0054	0.1413

Semi-trailer	ϵ_{p_2}	ϵ_{v_2}	ϵ_{a_2}	ϵ_{ψ_2}	$\epsilon_{\dot{\psi}_2}$	ϵ_{total_2}
Loaded	1.1685	0.0479	0.0144	0.1387	0.0037	0.2462
Unloaded	1.1110	0.0579	0.0275	0.1113	0.0050	0.2968

Articulation	ϵ_{γ_1}	$\epsilon_{\dot{\gamma}_1}$	ϵ_{total_γ}
Loaded	0.0324	0.0026	0.2347
Unloaded	0.0713	0.0032	0.3183

Overall	ϵ_{total}
Loaded	0.6409
Unloaded	0.7564

F Plots for Assessing the Model Accuracy

Global Velocity

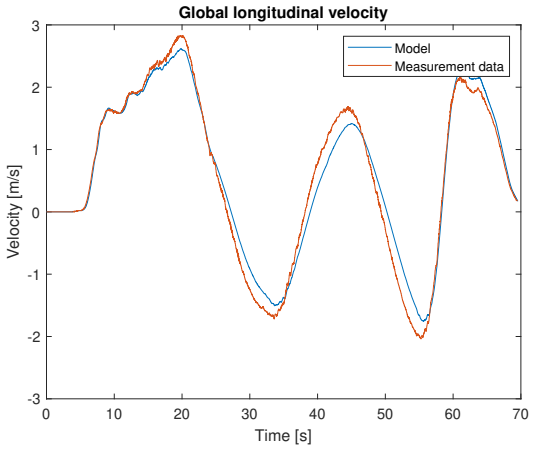

Figure F.1: Global velocity with highest error

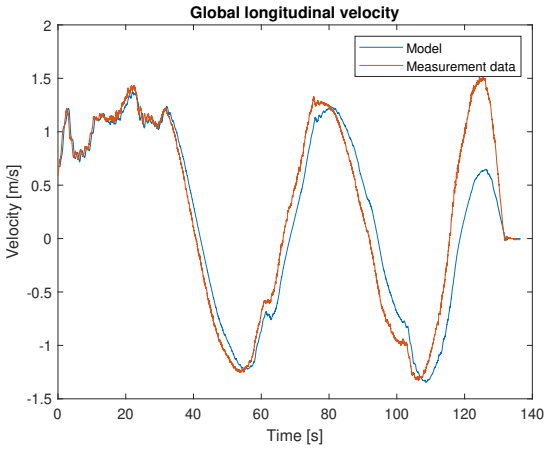

Figure F.2: Global velocity with average error

Local velocity

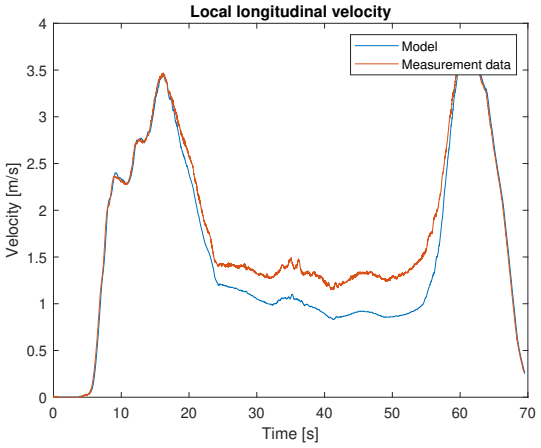

Figure F.3: Local velocity with highest error

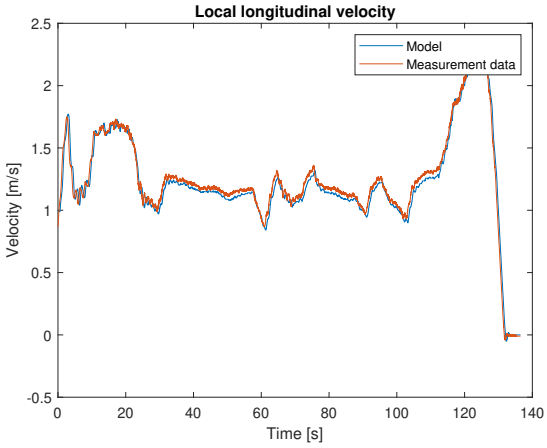

Figure F.4: Local velocity with average error

Acceleration

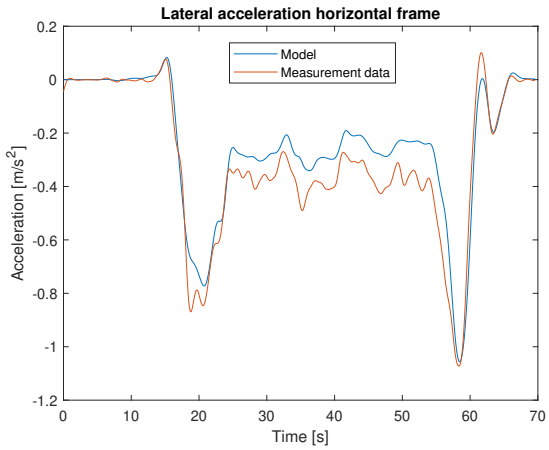

Figure F.5: Acceleration with highest error

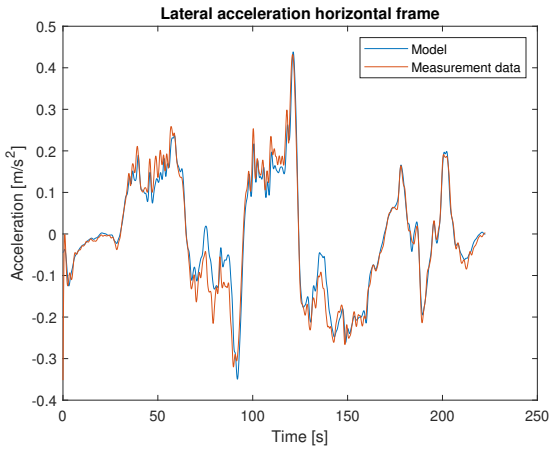

Figure F.6: Acceleration with average error

Yaw Acceleration Tractor

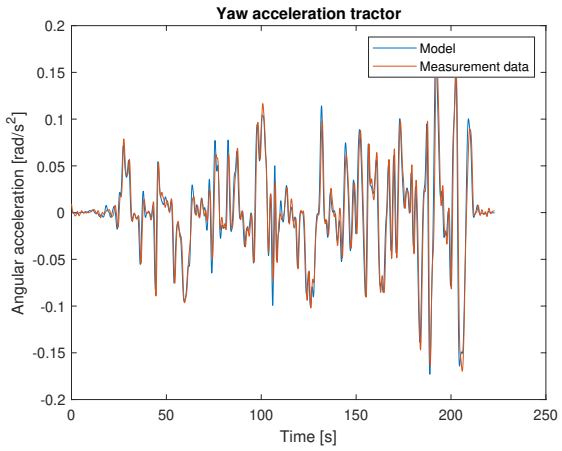

Figure F.7: Yaw acceleration tractor with highest error

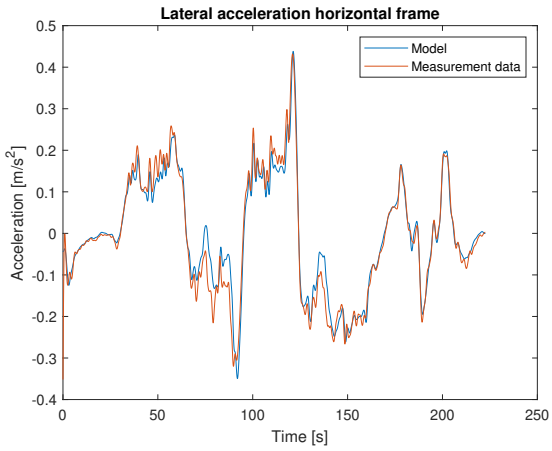

Figure F.8: Yaw acceleration tractor with average error

Yaw Acceleration Semi-trailer

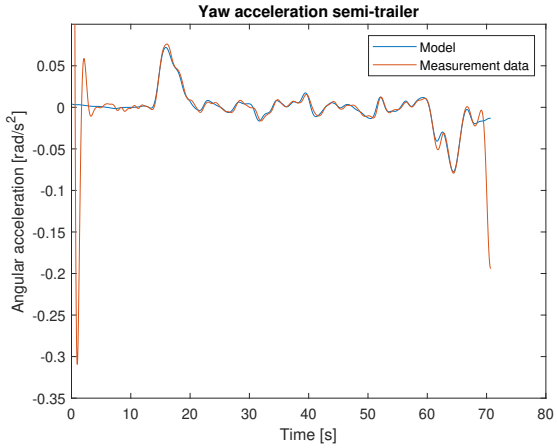

Figure F.9: Yaw acceleration semi-trailer with highest error

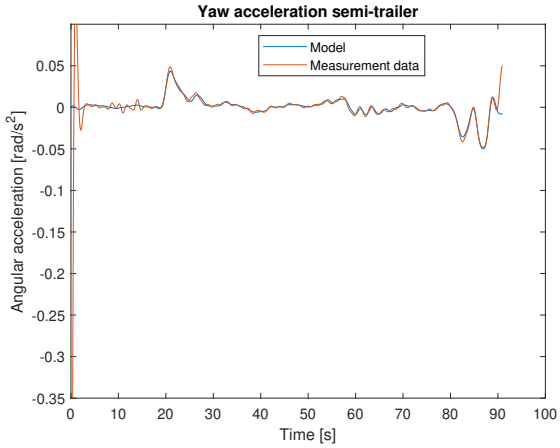

Figure F.10: Yaw acceleration semi-trailer with average error

G Simulink Model

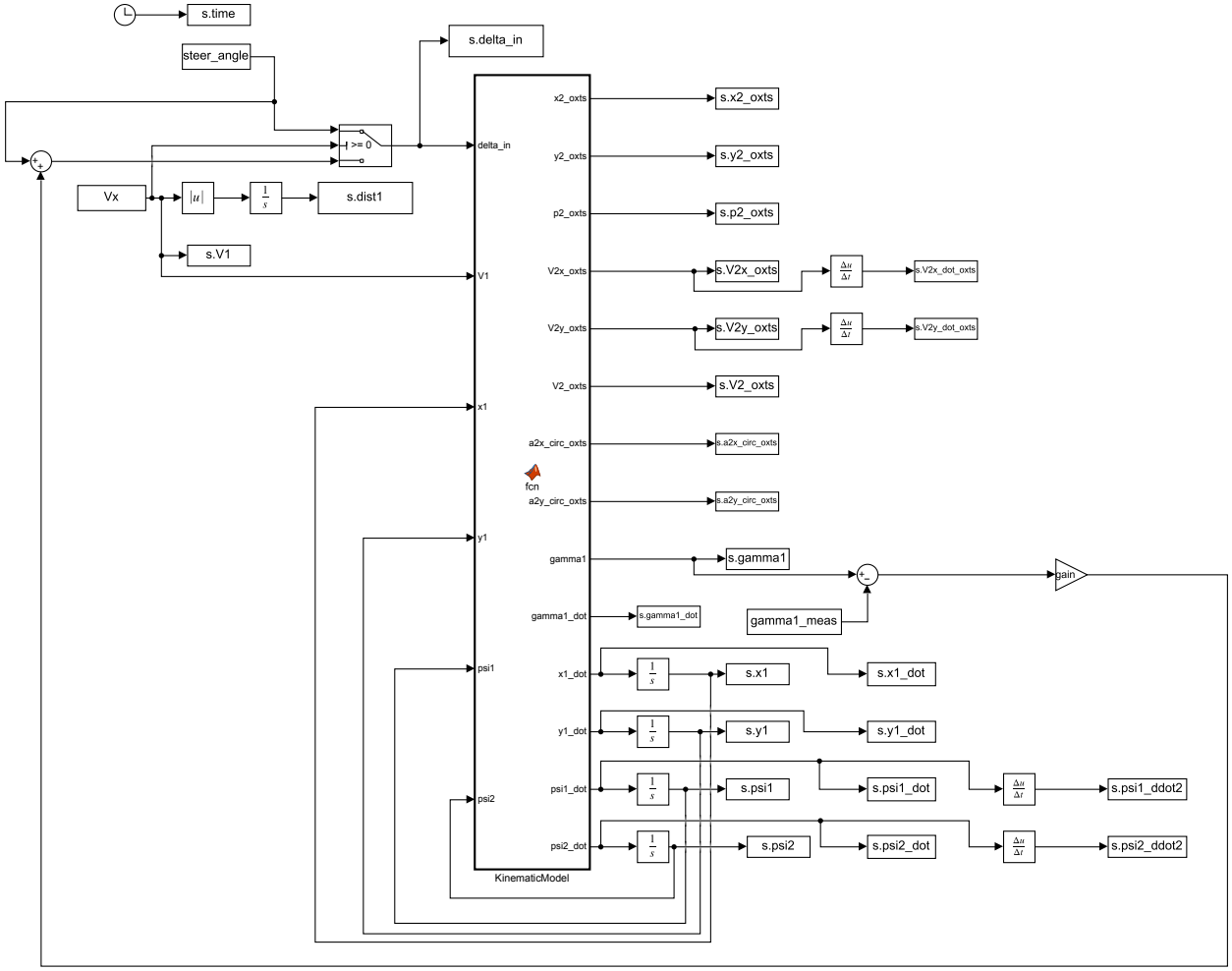

Figure G.1: Simulink model